ELSEVIER

PII: S0032-3861(96)00468-5

Polymer Vol. 38 No. 21, pp. 5379–5387, 1997

0032-3861/97/$17.00 + 0.00

Miscibility, thermal behaviour and morphological structure of poly(3-hydroxybutyrate) and ethyl cellulose binary blends

Lianlai Zhang*†‡, Xianmo Deng† and Zhitang Huang‡

† *Chengdu Institute of Organic Chemistry, Academia Sinica, PO Box 415, Chengdu 610041 and* ‡ *Institute of Chemistry, Academia Sinica, Beijing 100080, People's Republic of China*

(Revised 13 January 1997)

The miscibility, crystallization and melting behaviour, and phase morphology of poly(3-hydroxybutyrate) (PHB) and ethyl cellulose (EC) blends prepared by casting films have been studied by d.s.c., *FT*i.r., SEM and polarizing optical microscopy. The casting films of PHB/EC (60/40), (40/60) and (20/80) blends and annealed samples of the casting films of PHB/EC (80/20), (60/40), (40/60) and (20/80) blends showed composition-dependent glass transitions, the temperature position increased with the decrease of PHB content in the blends, and reached the maximum value for the EC component. After melt quenched or d.s.c. cooling run, only a lower glass transition temperature (T_g) corresponded to that of PHB phase in the blends was found in d.s.c. trace for each blends. The T_g remained almost unchanged at about 5 or 9°C. The hydrogen bonding of hydroxyl groups of EC was proved stronger than that of the hydroxyl group in EC with carbonyl group in PHB. The absorption bands of hydroxyl groups in EC decreased with the increase of PHB content in the blends, while the absorption bands of carbonyl groups in PHB were independent of the blend composition at 1723–1724 cm^{-1}. Unlike the PHB component, the blends displayed no crystallization when cooled from the melt during the d.s.c. non-isothermal crystallization runs. The cold crystallization peaks of the blends were presented in the following d.s.c. heating runs. The growth of PHB spherulites was delayed by EC content. Both the temperature and the heat of the cold crystallization (T_{cc} and ΔH_{cc}) were dependent on the blend composition. Higher T_{cc} and ΔH_{cc} of PHB/EC (80/20) blend than those of PHB component and other blends were found due to the stronger interaction between two components at this ratio. The T_m and crystallinity (C_r) of PHB in the PHB/EC (80/20) blend are higher than those of pure PHB in most cases because of the higher T_{cc}. No evidence of phase separation of the blends was observed by SEM studies. © 1997 Elsevier Science Ltd.

(Keywords: poly(3-hydroxybutyrate); ethyl cellulose; blend; miscibility; thermal behaviour; morphology)

INTRODUCTION

Bacterially produced poly(3-hydroxybutyrate) (PHB) has attracted much attention as a biodegradable thermoplastic polyester[1–8]. PHB can be degraded to water and carbon dioxide under environmental conditions by a variety of bacteria, and has much potential for applications of environmentally degradable plastics[9]. However, it suffers from some disadvantages compared with conventional thermoplastics, such as polyethylene (PE) and polypropylene (PP), for example, brittleness and narrow processability window[9–12]. To improve these properties of PHB, various copolymers containing hydroxyalkanoate units other than 3-hydroxybutyrate (3HB) units have been biosynthesized[8], for example poly(3-hydroxybutyrate-*co*-3-hydroxyvalerate) (PHBV) (trade name Biopol, ICI Biological Products)[1,9], poly(3-hydroxybutyrate-*co*-4-hydroxybutyrate) (P3HB-*co*-4HB)[13,14], and copolyhydroxyalkanoates with long-side-chains[15,16]. The composition of monomer units in these copolyesters can be controlled by using a mixture of carbon sources in the culture medium, thus the physical properties, such as melting temperature and crystallinity, vary widely[5]. However, both PHB homopolymer and copolymers are more expensive than conventional plastics[6,17]. Blending PHB with other polymers may offer opportunities to modify the physical properties, improve the processability and lower cost[18].

So far, many blends containing PHB have been studied, including binary blends with poly(ethylene oxide) (PEO)[19–23], poly(vinylene fluoride) (PVDF)[24,25], poly(vinyl acetate) (PVAc)[26], ethylene propylene rubber (EPR), ethylene-vinylacetate copolymer[26,27], polyepichlorohydrin (PECH)[28–30], poly(vinyl alcohol) (PVA)[31,32], poly(vinyl phenol) (PVPh)[33], poly(methyl methacrylate) (PMMA)[22,34–36], poly(cyclohexyl methacrylate) (PCHMA)[34], poly(L-lactide) (PLLA)[37], poly(D,L-lactide) (PDLLA)[38], poly(ε-caprolactone) (PCL)[39–42], synthetic PHB[43–45] and PHBV[46–49]. However, among these only PHB/PEO, PHB/PVA, PHB/PLLA, PHB/PDLLA, PHB/PCL, PHB/PHBV and PHB/synthetic PHB blends are biodegradable. Polysaccharide, such as cellulose and starch derivatives, another type of natural

* To whom correspondence should be addressed at: Department of Chemistry, National University of Singapore, Singapore 119260

polymer, is commercially available and also biodegradable. Scandola and co-workers have reported the miscibility, thermal and viscoelastic properties and biodegradation of PHB/cellulose acetate butyrate (CAB) and cellulose acetate propionate (CAP) blends[50–52]. Biodegradable natural composites containing PHB and cellulose fibre[53,54], PHB and straw fibre[55] have also been investigated by Gatenholm *et al.* and Avella *et al.*, respectively.

Over the years, we have focused on the biodegradable polymer blends containing PHB and PDLLA, PCL and poly(ester-ether)s[38,41]. The present work investigates the miscibility, thermal behaviour and morphological structure of PHB with ethyl cellulose (EC) blends.

EXPERIMENTAL

Materials

PHB, a kind gift from Chengdu Institute of Biology, Academia Sinica, was prepared via bacterial fermentation using methanol as carbon source by methylotrophic strain 8502-3 (*Hyphomicrobium zavarzinii* subsp. *chengduense* subsp. *nov.*)[56]. The crude product was dissolved in chloroform, filtered and then precipitated into methanol. The precipitate was filtered and dried under vacuum. The weight average molecular weight was 2.3×10^5 determined by intrinsic viscosity measurement using the relationship $[\eta] = 1.18 \times 10^{-4} \bar{M}_w^{0.78}$ in chloroform at 30°C[57]. Ethyl cellulose (EC) powder was a commercial product of the Chengdu Chemical Reagent Factory, with ethoxyl content 45–49%, viscosity 900 ± 1 cp. EC was first dissolved in chloroform, filtered to cast film from the filter liquor, dried at room temperature, and finally dried under vacuum. The weight average molecular weight was 1.7×10^4 according to the equation $[\eta] = 11.8 \times 10^{-3} \bar{M}_w^{0.89}$ measured in chloroform at 25°C[58].

Preparation of blends

Thin films of PHB/EC blends with weight ratios of 100/0, 80/20, 60/40, 40/60, 20/80, and 0/100 were prepared by casting from 3% (wt/v) solution of the two components in chloroform, allowing the solvent to evaporate at room temperature overnight, then keeping at 40°C under vacuum for 48 h. For annealing, the resultant films were maintained at 70°C for 10 days.

Differential scanning calorimetry (d.s.c.)

D.s.c. analysis was performed to study miscibility and thermal behaviour of the blends, on a Perkin–Elmer DSC 7 apparatus equipped with a PE 3700 data station. The apparatus was calibrated with indium standard and nitrogen atmosphere was used throughout.

Samples as casting films were first heated from −60 to 200°C at a heating rate of 20°C min^{-1} (I run). The melting temperatures (T_ms) and apparent enthalpy of fusion (ΔH_f) were determined from d.s.c. endothermal peaks. After 1 min, samples were then cooled to −60°C at a cooling rate of 100°C min^{-1} (II run). The III run was also a heating run at a rate of 20°C min^{-1} to 200°C, after 1 min followed by the IV run, cooling the samples to −60°C again at a rate of 20°C min^{-1}. And finally, the samples were reheated to 200°C (V run). The crystallization temperatures (T_cs) and heat of crystallization (ΔH_c) were determined from d.s.c. exothermal peaks in II and IV runs. The T_m, ΔH_f, cold crystallization temperatures (T_{cc}s) and heat of cold crystallization (ΔH_{cc}) were obtained from III and V runs.

The annealed samples were first heated to 200°C at a rate of 20°C min^{-1}, after 1 min rapidly quenched to −60°C to obtain melt quenched samples. The melt quenched samples were then scanned using I run condition. The T_m, T_c and T_{cc} were taken as the peak values of the respective endothermal and exothermal processes in d.s.c. curves. In the presence of multiple endothermal peaks, the maximum peak temperature was taken as T_m. The T_g was taken as the midpoint of the specific heat increment.

Fourier transform infrared spectroscopy (FTi.r.)

*FT*i.r. spectra were obtained with a Nicolet MX-1 i.r. spectrometer at room temperature. A total of 27 scans were taken with a resolution of 2 cm^{-1} in all cases. Samples were prepared by casting 3% (wt/v) solution directly onto KBr pellets, allowing the solvent to evaporate at room temperature, and then vacuum dried at 40°C overnight. After *FT*i.r. measurement, the pellets were heated to 190°C in an oven and then slowly cooled to room temperature over 8 h to obtain annealed samples for *FT*i.r. study.

Polarizing optical microscopy

A Leitz Wetzlar Ortholux II POL-BK microscope equipped with a hot stage was used to observe the crystallization and growth of spherulites of PHB in the blends. Samples cut from the casting films were first heated to 220°C, and then cooled rapidly to the desired temperatures, allowed to crystallize isothermally under crossed polars.

Scanning electron microscopy (SEM)

SEM was performed with an AMRAY 1000B equipment operated at 15 or 20 kV to examine the phase morphology. The blend films after methanol etching were used for surface observation. The fractured samples were prepared by submerging the casting films into liquid N_2, and being fractured. Before observation, all samples were coated with a thin layer of gold by means of a polaron sputtering apparatus.

RESULTS AND DISCUSSION

Blend miscibility

The thermograms of casting samples of the two components and the blends in *Figure 1*, show that PHB is a crystalline polymer with a melting point of about 175°C and a high crystallinity. No T_g of PHB is determined in d.s.c. trace by heating the casting film sample from −60 to 200°C (I run). In the thermogram of EC during the I run (*Figure 1* curve f), two main transitions appear at about 50–110°C and 155–185°C, corresponding to the glass transition and fusion process, respectively. Considering the very low crystallinity of EC, the fusion process will not be discussed in the present paper, and consequently the contribution to the endothermal peaks of PHB in the blends at almost the same region may be omitted. PHB/EC (60/40), (40/60) and (20/80) blends display single glass transitions during the I run, see *Figure 1* curves c to e. After annealing at 70°C, the blends show the same transitions with a small shift of the temperature position, as shown in *Figure 2*. The T_gs of the blends increase with the increase of EC

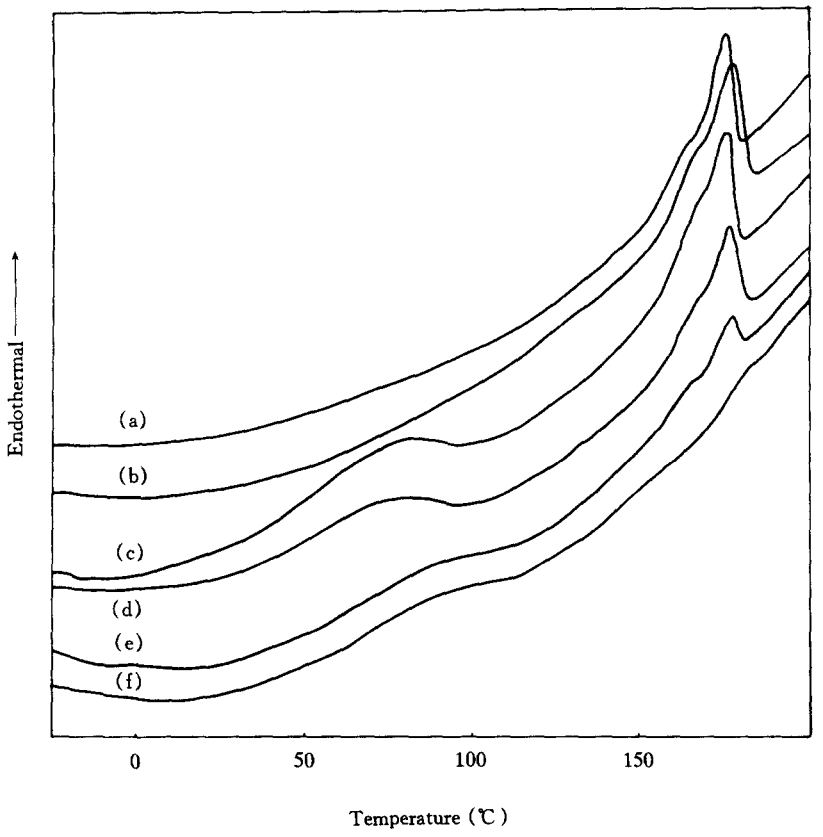

Figure 1 D.s.c. thermograms of casting samples: (a) PHB; (b) PHB/EC (80/20); (c) PHB/EC (60/40); (d) PHB/EC (40/60); (e) PHB/EC (20/80); (f) EC

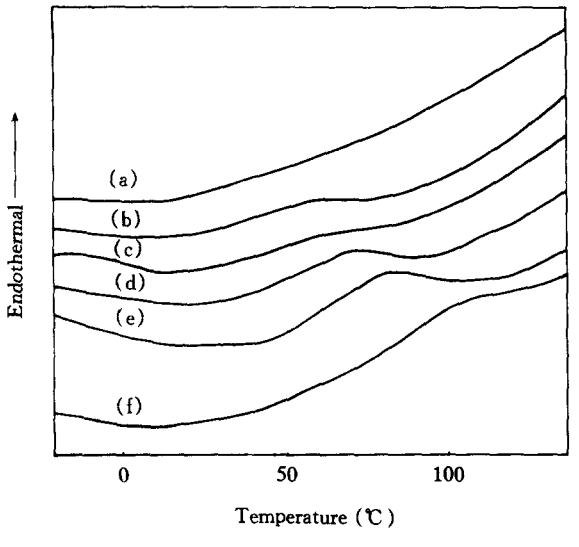

Figure 2 D.s.c. thermograms of annealed samples: (a) PHB; (b) PHB/EC (80/20); (c) PHB/EC (60/40); (d) PHB/EC (40/60); (e) PHB/EC (20/80); (f) EC

content. The specific heat (ΔC_p) of the T_g transition of the annealed samples also increases with the increase of EC content, as recorded in *Table 1*.

For melt quenched samples, both plain PHB and blends show glass transitions at about 5°C during a d.s.c. heating run related to the glass transition of the PHB component. Moreover, the ΔC_p decreases with the decrease of PHB content (see *Table 1*). Samples with different cooling history show small shifts in the T_gs as well as ΔC_p values. For samples after cooling from the melt at a rate of 100 or 20°C min^{-1}, the T_gs appear at about 9 and 7°C, respectively in d.s.c. heating runs. *Figure 3* gives the curves of a d.s.c. heating run for samples after cooling at a rate of 100°C min^{-1}. No T_g is determined from the melt quenched sample of EC, or after cooling runs from the melt at a rate of 100 or 20°C min^{-1}. Considering EC a thermotropic liquid crystal polymer[59], we can assume that supercooled liquid crystal may exist below T_g. After cooling from the melt, no T_g transition is found in the next heating runs.

Table 1 Glass transition temperatures (T_gs) and specific heat (ΔC_p) of plain PHB, EC and PHB/EC blends

Sample PHB/EC	T_g[a] (°C)	ΔC_p[a] (J·g^{-1}·°C^{-1})	T_g[b] (°C)	ΔC_p[b] (J·g^{-1}·°C^{-1})	C_r[b] (%)	X_{Aa}[c] (wt%)	q[d]
100/0	5.3	0.787	—	—	53.6	100	—
80/20	5.3	0.437	44.6	0.82	55.0	64.3	− 2.66
60/40	4.0	0.307	40.7	1.12	55.4	40.1	−71.5
40/60	5.6	0.230	50.0	1.30	48.4	25.6	−69.0
20/80	4.9	0.073	56.1	1.53	26.9	15.4	−77.1
0/100	—	—	70.4	2.30	0	0	—

[a] Obtained from melt quenched samples
[b] Obtained from annealed samples
[c] Calculated from equation (4)
[d] Calculated from equation (1)
—: not available

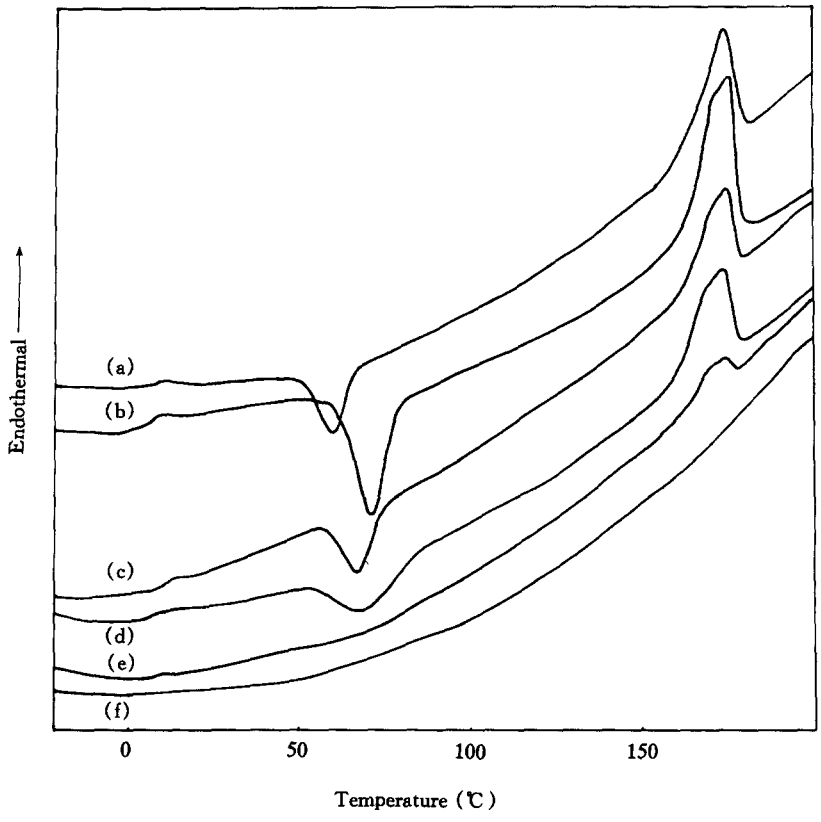

Figure 3 D.s.c. thermograms of samples after cooling run at a rate of 100°C min^{-1}: (a) PHB; (b) PHB/EC (80/20); (c) PHB/EC (60/40); (d) PHB/EC (40/60); (e) PHB/EC (20/80); (f) EC

Table 2 Values of the absorption frequency (cm^{-1}) of hydroxyl and carbonyl groups in PHB and EC

Sample	Casting sample			Annealed sample		
PHB/EC	ν_{O-H}		$\nu_{C=O}$	ν_{O-H}		$\nu_{C=O}$
100/0	—	3436	1725	—	3435	1724
80/20	3451	3436	1723	3445	3436	1723
60/40	3465	3436	1724	3468	3436	1723
40/60	3471	—	1724	3468	3437	1723
20/80	3474	—	1724	3472	—	1723
0/100	3478	—	—	3474	—	—

EC is a rigid polymer with some type of flexibility due to the hydrogen bonding of hydroxyls bearing on the backbone, while PHB has carbonyl groups, which are proton acceptors along the main chains. So, *FT*i.r. is used to examine the possible interaction between the two components. The absorption of hydroxyls in EC is broad, strong and symmetrical, centred at 3478 cm^{-1}, while the absorption of hydroxyl end groups of PHB is weak and sharper at 3436 cm^{-1}. Both absorptions of hydroxyls in EC and PHB are indicative of intermolecular hydrogen bonding. In PHB/EC blends, the O–H stretching bands of EC shift to lower frequencies, as shown in *Table 2*. The carbonyl regions show that C=O stretching bands of PHB are independent of EC content at 1723–1725 cm^{-1}, with shoulders at about 1740 cm^{-1}, which are representative of PHB crystalline and amorphous zones. After annealing, similar results are obtained at hydroxyl regions with some new features at carbonyl regions, as shown in *Figure 4*. The bands at 1724 cm^{-1} become broad and the intensity of the shoulders become lower, indicating that the crystallinity

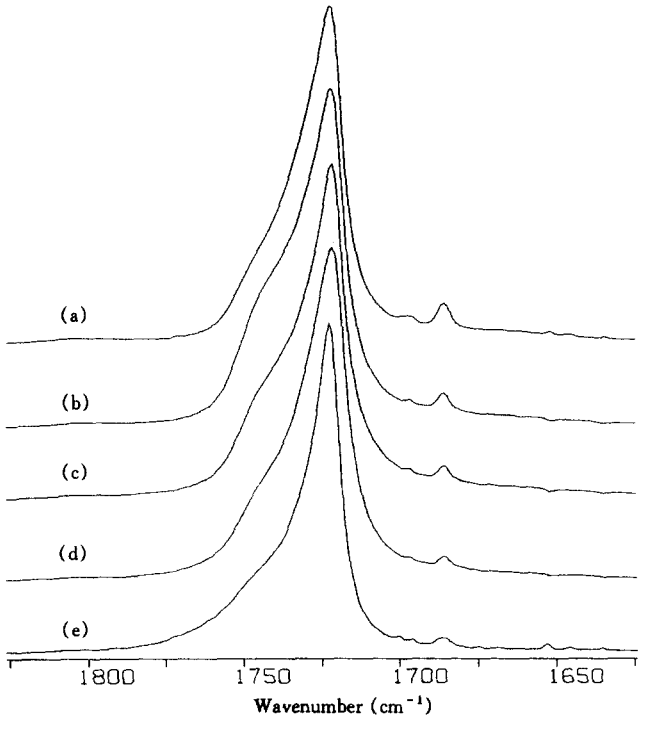

Figure 4 *FT*i.r. spectra in the region of 1825–1625 cm^{-1} of annealed PHB and PHB/EC blends: (a) PHB; (b) PHB/EC (80/20); (c) PHB/EC (60/40); (d) PHB/EC (40/60); (e) PHB/EC (20/80)

of PHB had increased during the thermal treatment. The *FT*i.r. results show that the hydrogen bonding in EC is stronger than that between EC and PHB chains. Thus, the T_g behaviour is the result of a balance between the

hydrogen bondings in EC component and in EC and PHB components.

The T_g behaviour of polymer blends is usually described by several equations, such as Fox, Gordon-Taylor and Couchman equations[60–62]. In systems with specific interactions, there are often deviations of composition dependence of T_g from that predicted by these equations. Equations derived by Kwei[63], Braun and Kovacs[64] have been used to represent these systems, respectively. Similarly, Painter *et al.* introduced a modified Couchman equation[65]

$$T_{gm} = (X_A T_{gA} + KX_B T_{gB})/(X_A + KX_B) + X_A X_B q \quad (1)$$

where X is the weight fraction, subscripts A, B and m denote the pure polymers and the mixture, respectively. K is the ratio of the specific heat increments on going from the glassy to the liquid state

$$K = \Delta C_{pB}/\Delta C_{pA} \quad (2)$$

q depends on the intermolecular interactions

$$q = q'_m(X) + q'_B(T) \quad (3)$$

where $q'_m(X)$ is a composition-dependent term that depends upon the balance of interactions (self-association vs. inter-association) in the system, while $q'_B(T)$ represents the contribution from the temperature dependence of the specific heat of the self-associating component. The $q'_m(X)$ term can be either positive or negative, depending upon the balance of self-association and inter-association interactions.

For the crystalline polymer blend, in general, phase separation may take place when one component crystallizes from the homophase mixture, and the crystalline phase is in equilibrium with the amorphous phase. Assuming that only the amorphous PHB is associated with EC in the blends, the weight fraction of amorphous PHB and EC in total amorphous phase, X_{Aa} and X_{Ba} is used rather than X_A and X_B in equation (1)

$$X_{Aa} = X_A(1 - C_r)/\{X_A(1 - C_r) + X_B\} \quad (4)$$

$$X_{Ba} = 1 - X_{Aa} \quad (5)$$

where the crystallinity of the EC phase is approximately zero, and C_r is the crystallinity of PHB phase

$$C_r = \Delta H_f/(X_A \times \Delta H_f^0) \times 100\% \quad (6)$$

where ΔH_f is the apparent enthalpy of fusion per gram of the blends, and ΔH_f^0 is the thermodynamic enthalpy of fusion per gram of completely crystalline PHB, $\Delta H_f^0 = 146\,J\,g^{-1}$ [66]. From the data in *Table 1*, the value of q for PHB/EC blends can be calculated using equation (1), where $T_{gA} = 278\,K$, $T_{gB} = 343\,K$, $\Delta C_{pA} = 0.787\,J \cdot g^{-1} \cdot °C^{-1}$, $\Delta C_{pB} = 2.30\,J \cdot g^{-1} \cdot °C^{-1}$ and $K = 2.92$ are used. For PHB/EC (80/20), (60/40), (40/60) and (20/80) blends q is -2.66, -71.5, -69.0 and -77.1, respectively, which is negative for all blend compositions and means that the interactions between chains of the different polymers (EC and PHB) are weaker than those between chains of the same polymer (EC) as shown by *FT*i.r. measurement. For PHB/EC (80/20) blend, q is higher than those of other blends, some degree of interaction between EC and PHB would be expected.

Crystallization behaviour

It is well known that PHB is a high crystalline polymer, which can crystallize when cooled from the melt even at a fast rate. The non-isothermal crystallization of PHB is dependent on the scanning rates. In the thermograms of PHB and PHB/EC blends during d.s.c. cooling run at a rate of $100°C\,min^{-1}$, as expected, the d.s.c. trace of plain PHB displays one exothermal peak at 67.2°C, with a lower heat of crystallization (ΔH_c) which indicates incomplete crystallization of PHB. No exothermic peaks corresponding to the crystallization of PHB are found in d.s.c. traces of PHB/EC blends. Similarly, during a d.s.c. cooling run at a lower rate ($20°C\,min^{-1}$), only the plain PHB crystallized, and the T_c and ΔH_c were higher than those in a cooling run at a rate of $100°C\,min^{-1}$, see *Figure 5*. In fact, a lower cooling rate allows a pure PHB sample to crystallize completely. The traces of PHB/EC blends with EC content of 40% and above at a d.s.c. cooling run are similar to that of plain EC at both cooling rates. From this result, we can conclude that the EC component may delay the crystallization of PHB in the blends.

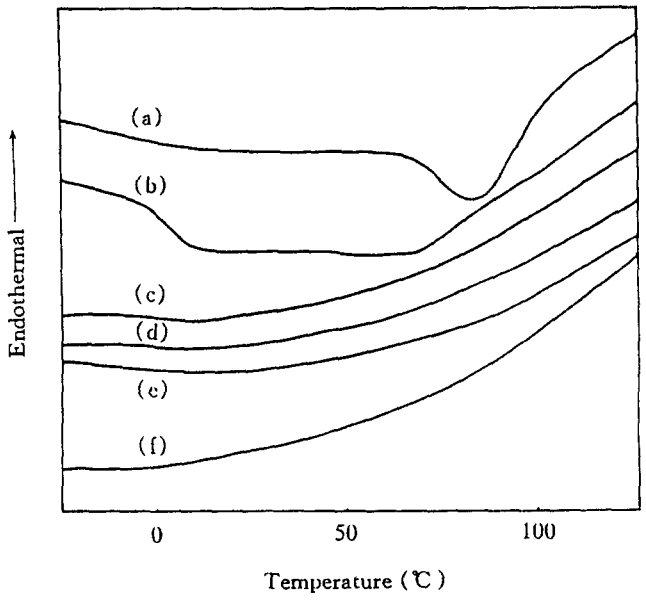

Figure 5 D.s.c. traces of cooling run at a rate of $20°C\,min^{-1}$: (a) PHB; (b) PHB/EC (80/20); (c) PHB/EC (60/40); (d) PHB/EC (40/60); (e) PHB/EC (20/80); (f) EC

Furthermore, the crystallization of PHB and PHB/EC blends were observed under crossed polars. The polarizing optical micrographs are shown in *Figure 6*. Well-defined spherulites were found growing rapidly at 100°C for plain PHB. However, no spherulite of PHB was observed for the blends at 100 or 80°C. Bright domains similar to liquid crystal texture were found for the blends and EC sample, and then small spherulites presented for PHB/EC (80/20), (60/40) blends over a long period of time. EC has been found to be a thermotropic liquid crystal polymer (transitions dependent on the ethoxyl content and preparing method)[59], though we have not found its liquid crystal phase transition from d.s.c. curve (*Figure 1*, curve f). The disc-shape domains of EC do not change until the temperature is under T_g, indicative of the formation of the supercooled EC mesophase. We may conclude that the crystallization of PHB follows the formation of EC mesophase. This is identical with that of no crystallization of PHB in the blends observed under non-isothermal processes. The results are related to the depression of the spherulite growth rate G of PHB due to

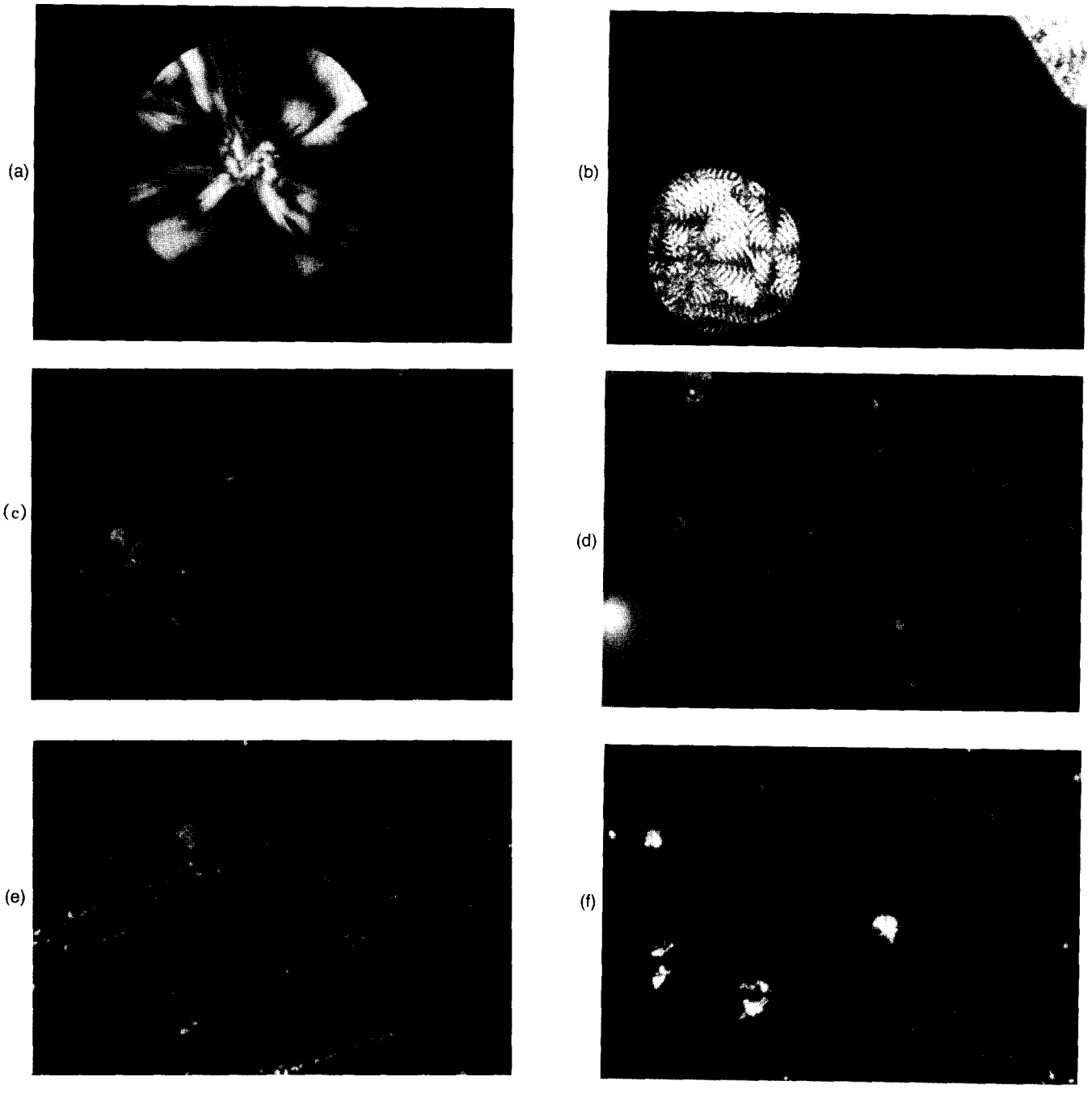

Figure 6 Polarizing optical micrographs of PHB, EC and PHB/EC blends under crossed polars: (a) PHB; (b) PHB/EC (80/20); (c) PHB/EC (60/40); (d) PHB/EC (40/60); (e) PHB/EC (20/80); (f) EC

the dilution effect of the EC component. However, this effect should not prevent completely PHB from crystallizing during non-isothermal crystallization runs, especially at a lower cooling rate (20°C min^{-1}). The influence of the melt miscibility on the primary nucleation processes should also be taken into account[67]. The crystallization behaviour can be explained only on the assumption that PHB crystallizes from a mixed phase, where the macromolecules of the two species are intimately intermingled. In totally miscible blends of PHB with cellulose acetate butyrate (CAB), the G of PHB markedly decreased in the presence of CAB, where 20 wt% of CAB caused a rate decrease of one order of magnitude[50]. It has also been found that no change in G of PHB spherulites and T_c occurred with increasing EPR content in PHB/EPR blends, where two components were immiscible in the melt[26]. So, the non-isothermal crystallization results imply that the PHB/EC blends are miscible in amorphous state. Similar behaviour has been found in miscible PHB/PEO, PHB/PVAc blends. Both the PEO and PVAc components caused drastic depression in G and T_c of PHB[19,26].

For PHB/EC blends with PHB content of 40% or above, cold crystallization peaks are found between T_g and T_m during the d.s.c. heating runs for melt quenched samples, or melt cooled samples (III and V runs), for example *Figure 3*. The cold crystallization temperature (T_{cc}) and heat of cold crystallization of PHB phase ($\Delta H_{cc}^{PHB} = \Delta H_{cc}/X_A$) are significantly dependent on the blend composition as shown in *Table 3*. Compared with that of plain PHB, the T_{cc}s of the blend samples shift to higher temperatures, indicative of difficulty in crystallization of PHB in the blends. This finding can also be explained by considering that the crystallization process

Table 3 Cold crystallization temperatures (T_{cc}s, °C) and heat of cold crystallization (ΔH_{cc}^{PHB}, J g^{-1}) of PHB and PHB/EC blends

Sample	I run[a]		III run		V run	
PHB/EC	T_{cc}	ΔH_{cc}^{PHB}	T_{cc}	ΔH_{cc}^{PHB}	T_{cc}	ΔH_{cc}^{PHB}
100/0	50.0	38.5	53.8	33.5	—	—
80/20	67.5	53.9	71.6	50.0	68.6	42.8
60/40	62.3	53.5	65.4	46.3	65.3	44.8
40/60	62.7	47.8	69.7	48.8	74.1	53.2

[a] Obtained from melt quenched samples

Table 4 Melting temperature (T_ms, °C) and apparent enthalpy of fusion (ΔH_f, J g^{-1}) of PHB and PHB/EC blends

Sample	I run		III run		V run	
PHB/EC	T_m	ΔH_f	T_m	ΔH_f	T_m	ΔH_f
100/0	175.3	76.8	173.0	69.2	169.8	73.1
80/20	177.0	67.5	175.5	62.2	174.2	70.8
60/40	175.0	45.3	173.8	42.2	171.1	46.3
40/60	176.0	22.3	173.5	27.4	169.0	28.4
20/80	176.0	9.0	170.0	11.2	170.0	11.1

takes place from a single homogeneous phase, in which the segment mobility of PHB chains is affected by EC chains, and the presence of the EC component causes a dilution of PHB nuclei. Both effects would result in a decrease in the overall crystallization rate and the increase of the cold crystallization temperature T_{cc}. On the contrary, in the case of two-phase PHB/*a*PMMA blends (cooled and annealed samples), as shown by Siciliano *et al.*[36], where the PHB component crystallized from its own phase, up to the (50/50) composition, the

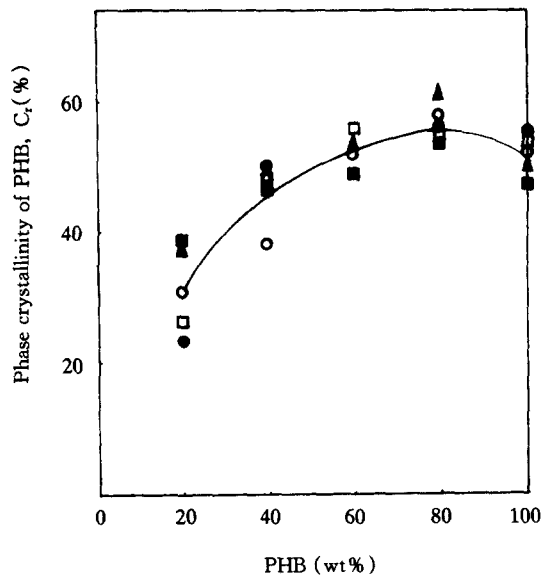

Figure 7 Crystallinity of PHB phase (C_r) as a function of the blend composition: (○) casting samples; (□) annealed samples; (●) melt quenched samples; (■) samples after d.s.c. cooling run at a rate of 100°C min^{-1}; (▲) samples after d.s.c. cooling run at a rate of 20°C min^{-1}. The line is drawn according to the average values of those of the five samples

crystallization did not suffer from the presence of *a*PMMA phase and the cold crystallization peak was present more or less at the same temperature. For PHB/*a*PMMA quenched samples, which were believed to be miscible, the T_{cc} moved toward higher temperatures with *a*PMMA component[36]. For PHB/EC (80/20) blend, the T_{cc} and ΔH_{cc} are higher than that of pure PHB and other

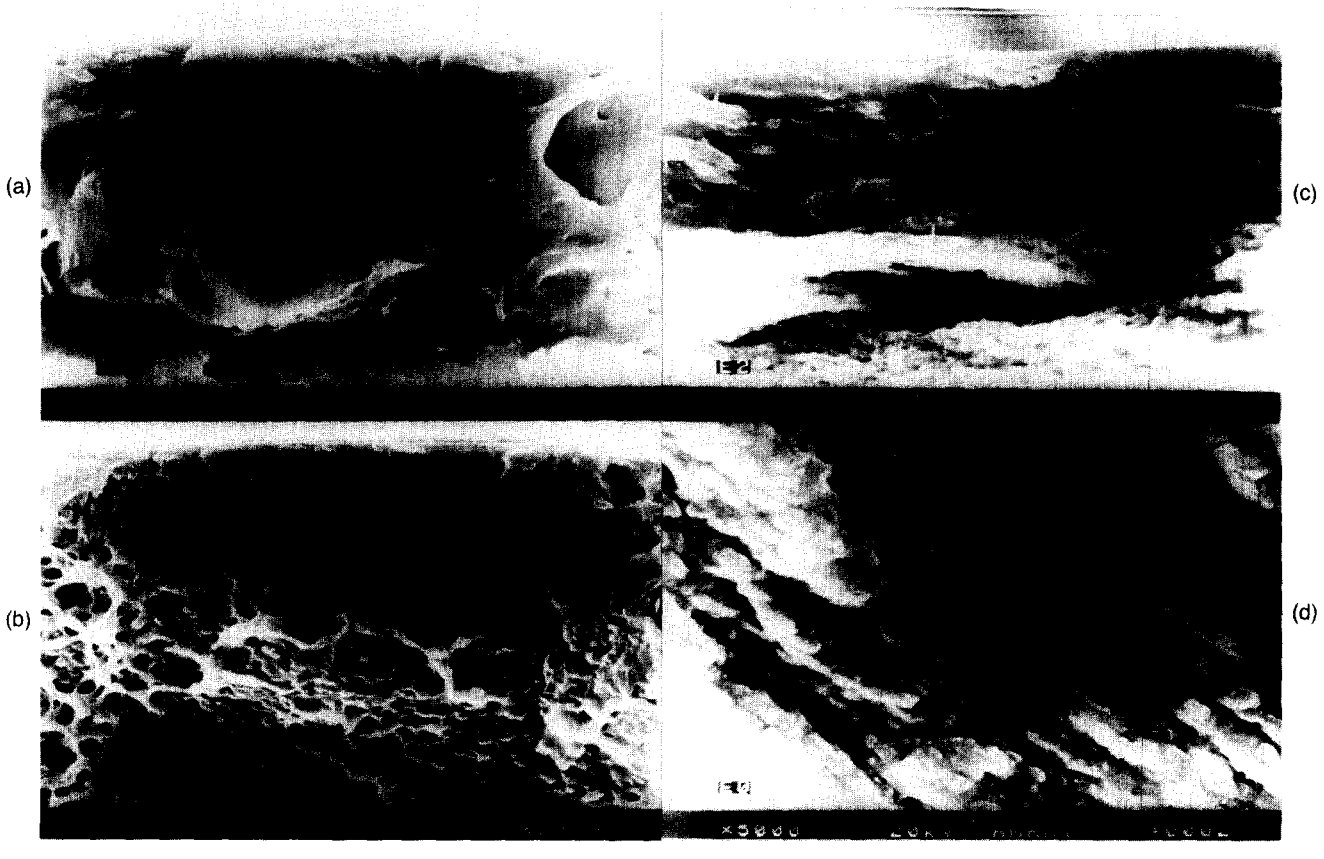

Figure 8 SEMs of PHB, EC and blends after fractured under liquid N_2: (a) PHB; (b) PHB/EC (80/20); (c) PHB/EC (20/80); (d) EC

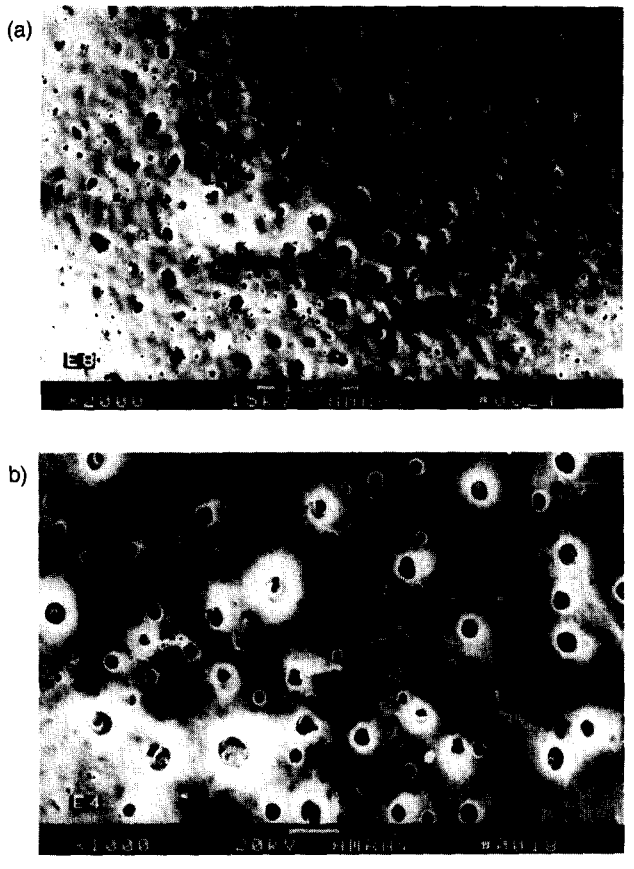

Figure 9 SEMs of PHB/EC blend films etched with methanol: (a) PHB/EC (80/20); (b) PHB/EC (40/60)

blends in most cases due to strong interaction between PHB and EC at the blend ratio.

Melting behaviour

Table 4 shows the data of melting process during d.s.c. heating runs. PHB and blend samples with different thermal history show T_ms at about 170–177°C, for example *Figures 1* and *3*. After a d.s.c. cooling run at a rate of 100 or 20°C min^{-1}, the T_ms of PHB in the blends decrease with the increase of EC content over the composition range of 20–30% PHB. Because the equilibrium melting points are not determined, it is difficult to draw a conclusion from the shifts of T_ms. However, we can obtain a clue to understanding the effect of the EC component on the fusion process of PHB. The T_m of the crystalline component in polymer blends, in general, depends on both morphological and thermodynamic factors[36]. The former is related to crystallization temperature, crystallization time, blend composition and scanning rate. Some of these factors can cause increase and/or decrease of T_m. In case of miscible blends, the thermodynamic factor must also be considered, whose contribution can only induce the decrease of T_m.

The apparent enthalpy of fusion of the blends, ΔH_f, which is related to the crystallinity of the blends shows significant depression with the increase of EC content. The crystallinity of PHB phase in the blends, C_r calculated by equation (6), shows a marked decrease when the EC content is 40% or above, as shown in *Figure 7*. It should be noted that the T_m and C_r of PHB in PHB/EC (80/20) blend are higher than those of pure PHB in some cases. The abnormal phenomenon can be explained from the study of crystallization behaviour. The higher T_{cc} of the PHB/EC (80/20) blend should cause the formation of crystals of PHB at higher temperatures, and hence higher T_m and C_r due to crystal morphology effects.

Morphology

SEM photographs of fracture surfaces of PHB, EC and PHB/EC (80/20), (20/80) blends in *Figure 8* show that the PHB/EC (20/80) blend has very smooth textures similar to a pure EC component, and PHB/EC (80/20) blend has a mottled aspect. No distinct phase boundaries are observed, which implies that no phase separation has taken place. *Figure 9* shows photographs of PHB/EC blends taken after methanol etching. It is found that the EC phase is uniform-distribution in the PHB phase.

CONCLUSIONS

The casting samples and annealed samples of PHB/EC blends displayed single composition-dependent T_gs, which increased with increase of EC content. However, the T_gs deviated from additive values of those of the two components, because the hydrogen bonding of hydroxyls in EC was stronger than that between hydroxyls in EC and carbonyls in PHB. The T_g behaviour was explained using a modified Couchman equation. No T_g of EC was determined from the melt quenched samples and melt cooled samples. The T_gs of PHB in the blends remained almost unchanged at about 5 or 9°C for melt quenched samples and melt cooled samples, respectively. Unlike the PHB component, the blends displayed no crystallization when cooled from the melt during d.s.c. non-isothermal crystallization runs. The growth of PHB spherulites from the melt under isothermal condition was also delayed by EC content. The cold crystallization peaks were dependent on the blend composition. The T_{cc}s of PHB in PHB/EC (80/20), (60/40) and (40/60) blends were higher than that of pure PHB. The interaction between EC and PHB in PHB/EC (80/20) blend was stronger than that in other blends, and consequently higher T_{cc}. The T_m and C_r of PHB in the PHB/EC (80/20) blend were also higher than those of pure PHB. No evidence of phase separation of blends was observed by SEM studies of fracture surfaces and methanol etching blend surfaces.

ACKNOWLEDGEMENTS

The authors are grateful to National Natural Science Foundation of China; Postdoctoral Science Foundation of China; and National Key Laboratory of Engineering Plastics, Institute of Chemistry, Academia Sinica, for financial support of this work. The authors also thank Professor Shujie Zhao of Chengdu Institute of Biology, Academia Sinica, for providing the PHB sample.

REFERENCES

1. Holmes, P. A., in *Developments in Crystalline Polymers*, Vol. 2, ed D. C. Bassett. Elsevier, London, 1988, pp. 1–65.
2. Doi, Y., *Microbial Polyesters*. VCH Publishers, New York, 1990.
3. Anderson, A. J. and Dawes, E. A., *Microbiol. Rev.*, 1990, **54**, 450.
4. Steinbüchel, A., in *Biomaterials*, ed. D. Byrom. Macmillan Publishers, London, 1991, pp. 123–213.
5. Inoue, Y. and Yoshie, N., *Prog. Polym. Sci.*, 1992, **17**, 571.

6. Hocking, P. J. and Marchessault, R. H., in *Chemistry and Technology of Biodegradable Polymers*, ed. G. J. L. Griffin. Chapman & Hall, London, 1994, pp. 48–96.
7. Sharma, R. and Ray, A. R., *J.M.S.–Rev. Macromol. Chem. Phys.*, 1995, **C35**, 327.
8. Doi, Y., *Macromol. Chem. Phys. Macromol. Symp.*, 1995, **98**, 585.
9. Holmes, P. A., *Phys. Technol.*, 1985, **16**, 32.
10. King, P. P., *J. Chem. Technol. Biotechnol.*, 1982, **32**, 2.
11. Howells, E. R., *Chem. Ind.*, 1982, **Aug.**, 508.
12. Barham, P. J. and Keller, A., *J. Polym. Sci. Polym. Phys. Ed.*, 1986, **24**, 69.
13. Kunioka, M., Kawaguchi, Y. and Doi, Y., *Appl. Microbiol. Biotechnol.*, 1989, **30**, 569.
14. Kunioka, M., Nakamura, Y. and Doi, Y., *Polym. Commun.*, 1988, **29**, 174.
15. Gross, R. A., DeMello, C., Lenz, R. W., Brandl, H. and Fuller, R. C., *Macromolecules*, 1989, **22**, 1106.
16. Marchessault, R. H., Monasterios, C. J., Morin, F. G. and Sundarajan, P. R., *Int. J. Biol. Macromol.*, 1990, **12**, 158.
17. Byrom, D., *Trends Biotechnol.*, 1987, **5**, 246.
18. Verhoogt, H., Ramsay, B. A. and Favis, B. D., *Polymer*, 1994, **35**, 5155.
19. Avella, M. and Martuscelli, E., *Polymer*, 1988, **29**, 1731.
20. Avella, M., Martuscelli, E. and Greco, P., *Polymer*, 1991, **32**, 1647.
21. Avella, M., Martuscelli, E. and Raimo, M., *Polymer*, 1993, **34**, 3234.
22. Yoon, J. S., Choi, C. S., Maing, S. J., Choi, H. J., Lee, H.-S. and Choi, S. J., *Eur. Polym. J.*, 1993, **29**, 1359.
23. Choi, H. J., Park, S. H., Yoon, J. S., Lee, H.-S. and Choi, S. J., *Polym. Eng. Sci.*, 1995, **35**, 1636.
24. Marand, H. and Collins, M., *ACS Polym. Prepr.*, 1990, **31**(1), 552.
25. Edie, S. L. and Marand, H., *ACS Polym. Prepr.*, 1991, **32**(2), 329.
26. Greco, P. and Martuscelli, E., *Polymer*, 1989, **30**, 1475.
27. Abbate, M., Martuscelli, E., Ragosta, G. and Scarinzi, G., *J. Mater. Sci.*, 1991, **26**, 1119.
28. Dubini Paglia, E., Beltrame, P. L., Canetti, M., Seves, A., Marcandalli, B. and Martuscelli, E., *Polymer*, 1993, **34**, 996.
29. Sadocco, P., Canetti, M., Seves, A. and Martuscelli, E., *Polymer*, 1993, **34**, 3368.
30. Sadocco, P., Bulli, C., Elegir, G., Seves, A. and Martuscelli, E., *Macromol. Chem.*, 1993, **194**, 2675.
31. Azuma, Y., Yoshie, N., Sakurai, M., Inoue, Y. and Chûjô, R., *Polymer*, 1992, **33**, 4763.
32. Yoshie, N., Azuma, Y., Sakurai, M. and Inoue, Y., *J. Appl. Polym. Sci.*, 1995, **56**, 17.
33. Iriondo, P., Iruin, J. J. and Fernandez-Berridi, M. J., *Polymer*, 1995, **36**, 3235.
34. Lotti, N., Pizzoli, M., Ceccorulli, G. and Scandola, M., *Polymer*, 1993, **34**, 4935.
35. Canetti, M., Sodocco, P., Siciliano, A. and Seves, A., *Polymer*, 1994, **35**, 2384.
36. Siciliano, A., Seves, A., De Marco, T., Cimmino, S., Martuscelli, E. and Silvestre, C., *Macromolecules*, 1995, **28**, 8065.
37. Blümm, E. and Owen, A. J., *Polymer*, 1995, **36**, 4077.
38. Zhang, L. L., Xiong, C. D. and Deng, X. M., *Polymer*, 1996, **37**, 235.
39. Gassner, F. and Owen, A. J., *Polymer*, 1994, **35**, 2233.
40. Lisuardi, A., Schoenberg, A., Gada, M., Gross, R. A. and McCarthy, S. P., *Polym. Mater. Sci. Eng.*, 1992, **67**, 298.
41. Zhang, L. L. and Deng, X. M. *Polym. Mater. Sci. Eng.* (in Chinese), 1994, **10**(1), 64.
42. Abe, H., Doi, Y. and Kumagai, Y., *Macromolecules*, 1994, **27**, 6012.
43. Pearce, R., Jesudason, J., Orts, W., Marchessault, R. H. and Bloembergen, S., *Polymer*, 1992, **33**, 4647.
44. Pearce, R., Brown, G. R. and Marchessault, R. H., *Polymer*, 1994, **35**, 3984.
45. Pearce, R. and Marchessault, R. H., *Polymer*, 1994, **35**, 3990.
46. Organ, S. J. and Barham, P. J., *Polymer*, 1993, **34**, 459.
47. Organ, S. J., *Polymer*, 1994, **35**, 86.
48. Satoh, H., Yoshie, N. and Inoue, Y., *Polymer*, 1994, **35**, 286.
49. Abe, H., Doi, Y., Satkowski, M. M. and Noda, I., *Macromolecules*, 1994, **27**, 50.
50. Scandola, M., Ceccorulli, G. and Pizzoli, M., *Macromolecules*, 1992, **25**, 6441.
51. Ceccorulli, G., Pizzoli, M. and Scandola, M., *Macromolecules*, 1993, **26**, 6722.
52. Tomasi, G. and Scandola, M., *J.M.S.–Pure Appl. Chem.*, 1995, **A32**, 671.
53. Gatenholm, P., Kubat, J. and Mathiasson, A., *J. Appl. Polym. Sci.*, 1992, **45**, 1667.
54. Gatenholm, P. and Mathiasson, A., *J. Appl. Polym. Sci.*, 1994, **51**, 1231.
55. Avella, M., Martuscelli, E., Pascucci, B., Raimo, M., Focher, B. and Annamaria, M., *J. Appl. Polym. Sci.*, 1993, **49**, 2091.
56. Zhao, S. J., Fan, C. Y., Hu, X., Chen, J. R. and Feng, H. F., *Appl. Biochem. Biotechnol.*, 1993, **39/40**, 191.
57. Akita, S., Einaga, Y., Miyaki, Y. and Fujita, H., *Macromolecules*, 1976, **9**, 774.
58. Brandrup, J. and Immergut, E. H., *Polymer Handbook*, 2nd edn. Wiley, New York, 1975, p. IV–33.
59. Chen, J., Huang, Y., Yuan, J., Yan, S. and Ye, H., *J. Appl. Polym. Sci.*, 1992, **45**, 2158.
60. Fox, T. G., *Bull. Am. Phys. Soc.*, 1956, **1**, 123.
61. Gordon, M. and Taylor, J. S., *J. Appl. Chem.*, 1952, **2**, 493.
62. Couchman, P. R., *Macromolecules*, 1978, **11**, 1156.
63. Kwei, T. K., *J. Polym. Sci. Polym. Lett. Ed.*, 1984, **22**, 307.
64. Braun, G. and Kovacs, A. J., in *Physics of Non-crystalline Solids*, ed. J. A. Prins. North-Holland, Amsterdam, 1965, p. 303.
65. Painter, P. C., Graf, J. F. and Coleman, M. M., *Macromolecules*, 1991, **24**, 5630.
66. Barham, P., Keller, A. J., Otun, E. L. and Holmes, P. A., *J. Mater. Sci.*, 1984, **19**, 2781.
67. Bartczak, Z. and Martuscelli, E., *Makromol. Chem.*, 1987, **188**, 445.